Indian Journal of Chemistry
Vol. 64, June 2025, pp. 627-633
DOI: 10.56042/ijc.v64i6.18325

Cyclic voltammetric analysis of pyrrole-N-vinyl carbazole copolymer and ZnO nanocomposite for the sensing of 6-TG

Kirtesh Pratap Khare
Department of Chemistry, Amity School of Engineering and Technology, Amity University, Gwalior 474 005, Madhya Pradesh, India
E-mail: kirteshkhare01@gmail.com

Received 27 March 2025; accepted (revised) 28 April 2025

Cyclic Voltammetry (CV) is an electro analytical technique that gives information about the redox behaviour of the analyte at a particular interface. Conducting polymers (CPs) are much explored sensor materials due to their unique properties such as, tunable conductivity, structural versatility, stability and multiple synthetic pathways. In the present work, investigations on the sensing ability of neat copolymer (Py-NVK) and ZnO nanocomposite (Py-NVK_ZnO) for 6-thioguanine (6-TG) anti-cancer drug molecule through the cyclic voltammetry method have been reported. The investigations have revealed that the ZnO nanocomposite is a better sensor material in terms of current-voltage for the detection of 6-thioguanine anti-cancer drug molecule in comparison to neat copolymer.

Keywords: Py, NVK, Copolymer, 6-TG, CV, Composite

Oxidation-reduction potentials of biological significance have long been a research area of imperative interest[1–5]. Considerable importance has been given to the search for consistent relationships involving the $E_{1/2}$ values and the structural characteristics of electro oxidizable and electro reducible substances. Actual biological redox systems are complex enzymatic progressions, characteristic pathways may be obtained in the laboratory through their redox intensities. Hydrogen ion potential in the acid-base equilibria remain important in biological systems. Accurate, economical and simple electroanalytical methods for drug residue monitoring and control have emerged through advance research[6–8].

Voltammetry involves the electrolysis of an analyte to work out the relationships of cell current with voltage/time. The electrolytic cell comprises a three-electrode assemblage, working electrode furnishing the heterogeneous interface, reference electrode deployed to manage the working electrode potential and an auxiliary electrode to carry current with the working electrode (shown in Fig. 1), With dropping mercury heterogeneous interface as working electrode and a pool of mercury as the auxiliary electrode, the technique in particular is referred as polarography.

To study the redox behaviour of biologically active compounds, polarography and cyclic voltammetry are predominantly useful methods[9].

In the present work, the synthesis of an electroanalytical method-based sensor material has been reported for the detection and quantification of 6-thioguanine anti-cancer drug molecule. For testing the utility of neat and ZnO nanocomposite, a Glassy Carbon Electrode (GCE) has been adapted with the synthesized materials to yield a sensor for electrochemical determination of 6-thioguanine. The electrode modifier nanocomposite intensifies the electron transfer rate in the diffusion-controlled electrode process to furnish enhanced and non-overlapping discrete peaks for the desired detection, determination, validation and quantification of 6-thioguanine. The enhanced efficacy of the modified nanocomposite has been established in comparison to the standard glassy carbon electrode as well as neat copolymer modified glassy carbon electrode.

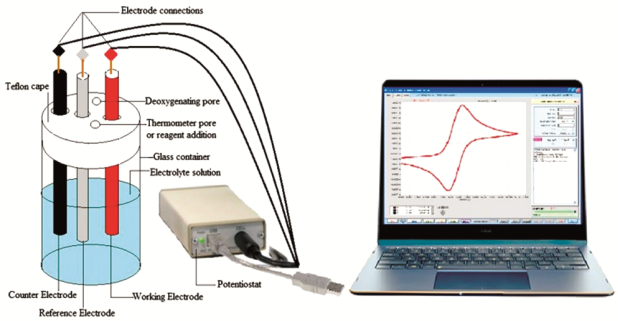

Fig. 1 — Typical cyclic voltammetry setup[16]

Cyclic Voltammetry

Cyclic voltammetry provides insight on thermodynamic redox systems, kinetics of heterogeneous electron transfer systems and coupled chemical reactions[10]. The characteristic shape of voltammetric curves with explicit position on the potential scale effectively fingerprint the electrochemical redox process (Fig. 2)[11].

In cyclic voltammetry, the working electrode potential is managed against the reference electrode. Employed as the excitation signal, the controlling potential is a linear scan adapting a triangular wave form. The triangular wave is imposed on a heterogeneous electrode interface. Forwards and converse processes are observed and the current potential characteristics of the concerned redox system are obtained[12]. Repetition of the triangular potential excitation signal on the working electrode with two fixed switching potentials is accomplished. The cyclic technique is advantageous for the investigation of unstable products, intermediates or radicals, especially in organic electrochemistry and coordination chemistry. The intermediates formed in the cathodic polarization can be detected from the anodic currents at higher scan rates. The equation of the diffusion controlled current in single sweep voltammetry was solved by Randles and Sevcik for the case of linear diffusion[13]. The most exhaustive derivation of single and cyclic sweeps with coupled chemical reactions has been developed by Nicholson and Shain[14].

E_p, the peak potential corresponding to the maximum current i_p characterizes a cyclic voltammogram. For reversible redox processes, peak current is obtained as:

$$i_p = 0.4463\ nF\ ADa^{1/2}\ C^*$$

From the set of differential equations for Fick's law of diffusion:

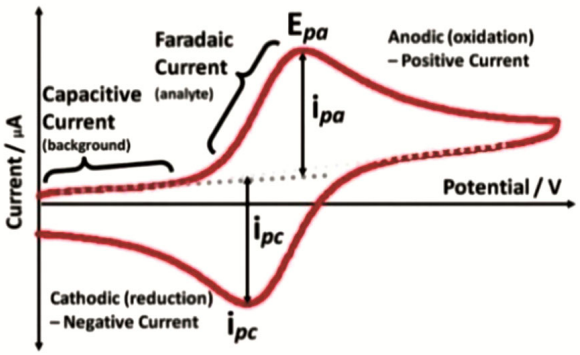

Fig. 2 — A typical cyclic voltammogram

$$D_a = \frac{nF\nu}{RT} = \frac{n\nu}{0.026} \text{(at 298.15 K)}$$

Thus, with variable constraints, the peak potential may be calculated by Randle -Savcik equation:

$$i_p = 2.69\times10^5 n^{3/2} A\ DA^{1/2}\ C^*\ \nu^{1/2}$$

Here, i_p is the current in ampere, 'A' is the electrode area in cm^2, D_A is the diffusion coefficient of the analyte A in cm^2/sec, C* is the concentration of analyte in mol/cm^3 and ν is the sweep rate in Volts/sec. According to this equation, i_p is proportional to $\nu^{1/2}$ and a plot of i_p *vs.* $\nu^{1/2}$ should be a straight line for a reversible system. The current maxima for reversible reaction is represented as heterogeneous rate constant $k_{f,h}$.

$$i_p = 0.227\ n\ FAC\ k_{f,h}\ e^{\left(\frac{\alpha nF}{RT} - (E_p - E)\right)}$$

Where, E is the potential corresponding to the measured current.

The peak potential for the reversible system is defined by the expression:

$$E_p = E°_{O,R} - \frac{0.029}{n} \text{(at 298.15 K)}$$

Where, E_p and $E^o_{O,R}$ are expressed in volts and $E^{\circ}_{O,R}$ is the formal electrode potential corrected to the reference electrode being used. When both the species in the redox couple readily exchange charge on the working electrode, it is termed as reversible electrochemical couple. Redox couples are recognized in a cyclic voltammogram by measuring the potential difference between the E_{pa} and E_{pc}.

$$\Delta E_p = E_{pa} - E_{pc} = \frac{0.059}{n}$$

Where, n is the number of electrons taking part in the electrode process, E_{pa} and E_{pc} are the anodic and cathodic peak potentials in volts. 0.059/n volts peak separation does not independent on scan rate in a reversible case. The potential central to E_{pa} and E_{pc} is the recognized electrode potential of the couple.

$$E^\circ = \frac{Epc - Epa}{2}$$

On increasing the scan rate ν, i_{pa} and i_{pc} show linear relation to $\nu^{1/2}$. For a reversible couple plot of i_{pa} and i_{pc} *vs.* $\nu^{1/2}$ are linear with intercept at the origin. The ratio of i_{pa} and i_{pc} is unity for a reversible couple, provided there are no kinetic complications.

$$\frac{i_{pa}}{i_{pc}} = 1$$

The half wave potential for a reversible system is related to the polarographic $E_{1/2}$ as:

$$E_{p/2} = E_{1/2} \pm \frac{28.0}{n} \text{ mV}$$

Owing to dynamic nature of cyclic voltammetry, irreversible processes give an expression for the peak current distinctly different from those of the reversible systems.

$$i_p = 2.99\times10^5 \, n \, (\alpha_{n_a})^{1/2} \, A \, D^{1/2} \, C^* \nu^{1/2}$$

Where, n_a is the number of electrons involved in the rate determining step of the electrode process and α is the transfer coefficient. These quantities can be evaluated by the following equation:

$$E_p - E_p^{1/2} = - 1.857 \frac{RT}{\alpha_{n_a}} = -1.857 \frac{0.026}{\alpha_{n_a}}$$

When the electron transfer is totally irreversible or rate of electrochemical step is much larger than the rate of chemical reaction, the reverse peak is not observed. If a post electron transfer process destroys the product before the reverse scan occurs, cathodic peak current and the anodic peak will have ratio greater than unity.

Experimental Section

The developed electrodes were assessed through cyclic voltammetry (CV). 6-TG drug was measured over the neat copolymer (Py-NVK) and ZnO nanocomposite (Py-NVK_ZnO) modified Glassy carbon electrode (GCE) with phosphate buffer solution, 0.1 M, *p*H 8.2 as the supporting electrolyte.

CV was carried out using Potentiostat Versastat EG & G II Princeton Applied Research Model 273 sufficed with 270/250 research electrochemistry software 4.30. Glassy carbon working electrode (ϕ = 2mm EG & G/PAR), Ag/AgCl reference electrode and Platinum wire auxiliary electrode comprised the electrodic assembly. Dissolved oxygen was appropriately eliminated with pure nitrogen. Bare GCE was refined with emery paper and polishing alumina (0.5μm), cleaned and activated for 5 minutes by cuneate voltage sweeps between +1.0 to –1.0 V at 5 to 200 mV/sec scan rate. Ferricyanide-ferrocyanide system in 0.1 M KCl was used to verify Electrode parameters.

Influence of various buffers (phosphate, acetate and Britton-Robinson) was compared for the analytical signals and it was observed that the diffusion current peaks were sharp and well defined in Phosphate buffer solution (PBS). PBS was used for maintaining 8.2 *p*H. The effect of the increase of depolarizer concentration at various *p*H and pulse amplitudes was studied. Electrodic runs were followed by recording UV-Visible spectra of the sample at different time intervals amidst electrolysis.

Modification of GCE with Neat Copolymer and ZnO nanocomposite

Glassy carbon electrodes (GCEs) were ultrasonically cleaned after polishing. Neat copolymer and ZnO nanocomposite were transformed into suspensions (100 mg/mL in DMSO). Surface modification of prepared GCEs was accomplished by plummeting 0.2 μL of the pre-formed suspensions on it. It was dried in room ambience.

Preparation of 6-TG Drug Sample

To assess the performance of the modified sensor for the chosen drug sample, electrodic quantification of 6-TG was performed. 6-TG drug (Cat No.: BD2698-5G, Lot No. BRW636, CAS 154-42-7, MW 167.19, Purity 98%) was procured from BLD Pharmatech (India) Pvt. Ltd, Hyderabad. [ISO 901: 2015 Certified]. 25 mL of 1M NaOH was used to dissolve 4.17 g of the 6-TG powder. With 0.45 mm grade filtration and serial dilution technique, concentration range upto 0.1 μM/L of the analyte solution obtained.

Results and Discussion

Optimization of Py-NVK/GCE and Py-NVK_ZnO/GCE

Carefully chosen parameters *viz*. *p*H and depolarizer concentration were optimized for studying the electrode reactions. Fig. 3a represent the variation in current response of Py-NVK_ZnO/GCE for 6-TG electrolysis in the range *p*H 5 to 10. It was observed that the oxidation of 6-TG favors *p*H 8.2 as evident by the corresponding increase in anodal current peak with *p*H towards the basic range. The peak current declined with increase in basicity beyond *p*H 8.2. This behaviour of the depolarizer may be related with the structural changes in the 6-TG molecule beyond *p*H 8.2.

0.1 – 0.5 μM/L depolarizer concentration range was also studied for the best analytical signal. Fig. 3b increase in the current response up to 0.37 μM/L concentration of the depolarizer was recorded on Py-NVK_ZnO modified GCE. Decrease in current density beyond 0.4 μM/L can be associated with the steric interference to the 6-TG molecules diffusing towards the electrode interface. Thus, 0.37 μM/L was selected as the optimal concentration of the depolarizer.

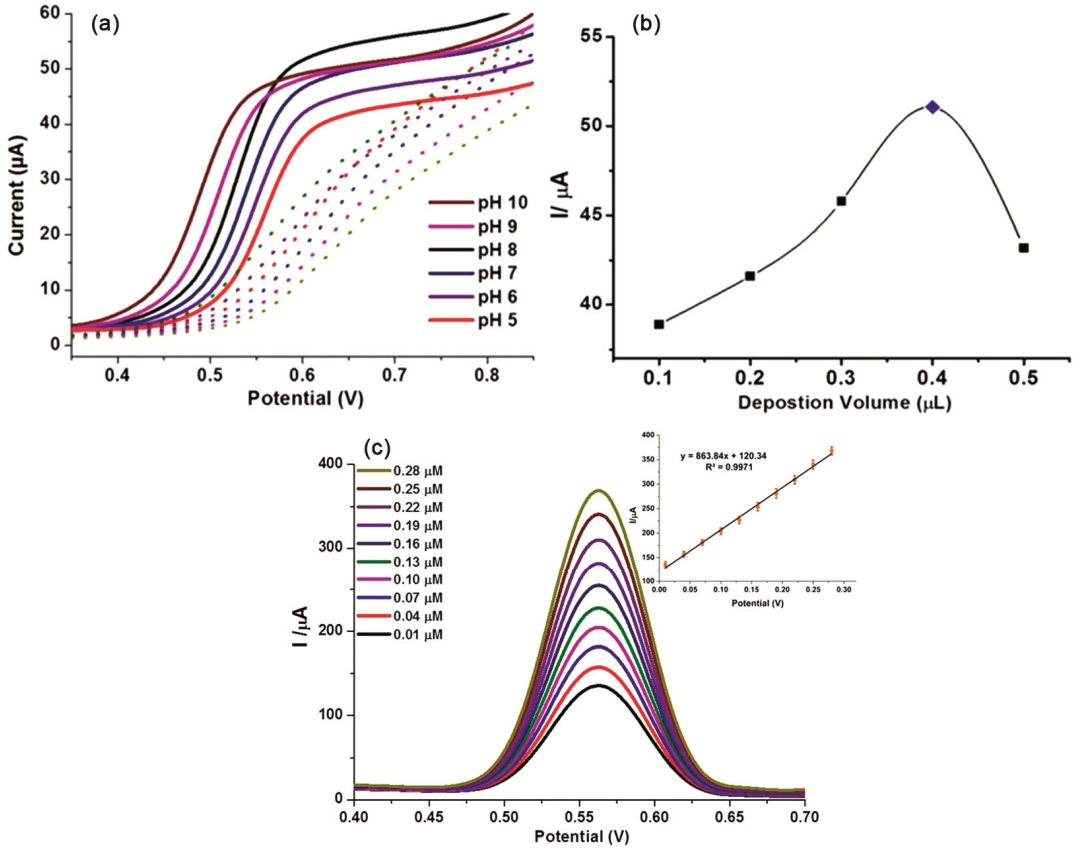

Fig. 3 — (a) *p*H optimization, (b) Depolarizer concentration optimization, (c) Linear current response for the depolarizer concentration 0.01 μM/L to 0.3 μM/L

Competence and Constancy of the sensor

6-TG drug was put to electrolysis in 0.01 – 0.30 μM/L samples to check the linear current response of the depolarizer under the same set of parameters (Fig. 3c).

Detection and quantification limits of 6-TG for the formulated electrode were appraised as 0.001 and 0.029 μM/L respectively. Sturdiness of modified interface was ascertained by studying the change in current flow for Py-NVK/GCE and Py-NVK_ZnO/GCE in 0.01 μM/L 6-TG drug in 0.1 M PBS, *p*H 8.2, post shelf life of 10 days and 1 month. With designated time lapse, insignificant disparity was experiential in the electrode signal which reflects the sturdiness of the modified sensor.

Fig. 4 shows the electrochemical characteristics of 6-TG 0.01 μM/L in 0.1 M PBS of *p*H 8.2 on bare GCE and the corresponding modified electrode responses as overlaid graphs. Bare GCE furnishes insignificant progress of 6-TG oxidation. Py-NVK_ZnO/GCE exhibited substantial current advance with anodal peak at 0.58 V. Anodal current

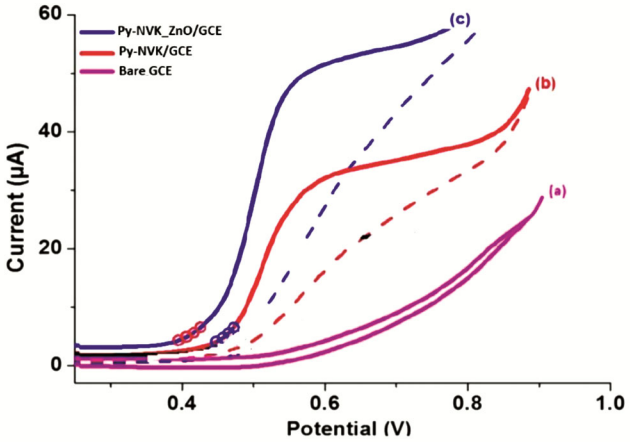

Fig. 4 — CV profile for modified electrode: Oxidative peak at 546 mV for 6-TG response of (a) bare GCE (b) Py-NVK/GCE and (c) Py-NVK_ZnO/GCE evaluated for 0.01 μM/L 6-TG in 0.1 M Phosphate buffer

peak was recorded for Py-NVK_ZnO/GCE against 0.01 μM/L 6-TG in 0.1 M PBS of 8.2 *p*H. Current response of Py-NVK_ZnO nanocomposite is precisely improved with increment in current

strength of ΔIp = 31.86 μA (Fig. 4). The enhanced current signal can be attributed to improved electronic properties of the nanocomposite providing easier mobility of charge facilitated by the presence of nano ZnO between the pyrrole and vinylcarbazole moieties enhancing interaction with the functional groups of 6-TG. This enablement, synergized with the greater surface expanse of the nanocomposite, results in improved response of 6-TG.

To understand the role of nano ZnO as dopant in the synthesized copolymer for enhanced electrostatic interaction in the reaction under investigation, the electrode process also assessed using neat Py-NVK modified GCE under same experimental parameters as optimized for Py-NVK_ZnO/GCE. Mentioning Fig. 5a-c, the Py-NVK/GCE responds with relatively smaller current compared to Py-NVK_ZnO/GCE (ΔIp = 22.47 μA). The current intensities observed for Py-NVK/GCE and Py-NVK_ZnO/GCE provide substantial indication for the contribution of advantageous interactions prevailing between the Py-NVK_ZnO and 6-TG molecules at the heterogeneous interface facilitating diffusion-controlled oxidation of the analyte. Interestingly, the current response of Py-NVK_ZnO/GCE is appreciably better compared to neat Py-NVK modified GCE reported in Table 1. This may be explained on the basis of the enhanced electronic properties associated with the Py-NVK_ZnO/GCE due to functionalizing with nano ZnO (Fig. 6a-d).

Chronoamperometry Measurements

Electrode potential of 0.65 V and 0.35 V as first and second potential step for diverse 6-TG solutions *viz*. 0.1–0.5 μM/L in 0.1 M PBS were employed to study the chronoamperometric depolarizer behaviour on Py-NVK_ZnO/GCE as shown in Fig. 6a. Diffusion coefficient 'D' was calculated using the Cottrell equation. Plots of peak current I against $t^{1/2}$ were optimized. Corresponding slopes when plotted against concentration of 6-TG as depicted in Fig. 6b. Fig. 6c demonstrates the linear fit of corresponding slopes plotted against 6-TG concentration; the slope of the final graph was further used to estimate the diffusion coefficient 'D' with the Cottrell equation as utilized below:

$$I = nFAD^{1/2}C_b\pi^{-1/2}t^{-1/2} \quad \ldots (1)$$

$$D = \left(\frac{m}{nFAC_b\,\pi^{-1/2}}\right)^2 \quad \ldots (1)$$

Here, m is the slope from the plot shown in Fig. 6c, whereas n is the number of electrons taking part in the electrodic oxidation[15], 'A' represents the area of GCE (0.07 cm^2) and C_b is the concentration of 6-TG in the bulk of the solution. F is Faraday constant. The value of D for Py-NVK_ZnO/GCE was estimated to be 1.68×10^{-4} cm^2/s. This noticeable diffusion constant can be ascribed to the high electronic properties of the modified electrode interface endorsing better analyte diffusion through the Hamiltonian double layer. The rate constant 'k' for the electro-oxidation of 6-TG at Py-NVK_ZnO/GCE was estimated using Galus equation:

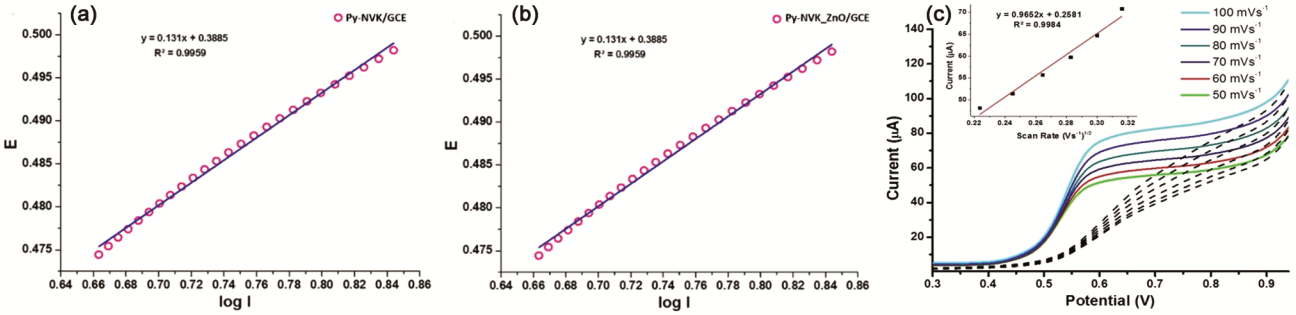

Fig. 5a-c — Tafel slopes devised from the current density plots of (a) Py-NVK/GCE and (b) Py-NVK_ZnO/GCE (c) Cyclic voltammograms of 6-TG at *p*H 8.20, conc. 0.01 μ M/L at scan rates range 50 –100 mV/s in 0.1 M PBS. Inset shows linear relationship of current intensity and square root of the corresponding scan rate

Table 1 — Cyclic Voltammetric Characteristic i_p for 6-TG at Py-NVK and Py-NVK_ZnO Modified GCE

R	Conc.×10^{-2} M	i_p (in μA) of Bare GCE	i_p (in μA) of Py-NVK/GCE	i_p (in μA) of Py-NVK_ZnO/GCE
6-TG	1.0	17.6	23.6	23.8
6-TG	2.0	27.8	32.8	33.5
6-TG	2.5	29.6	34.6	36.2
6-TG	3.0	32.6	36.6	38.7

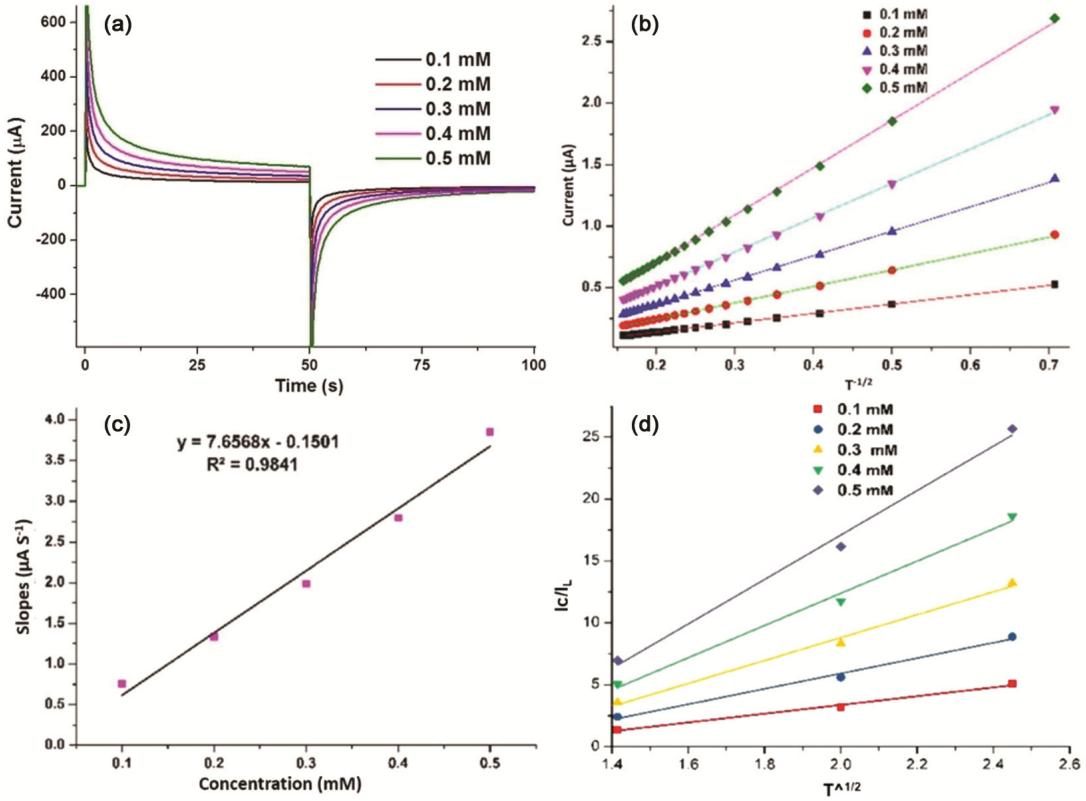

Fig. 6 — (a) Chronoamperometric measurement for Py-NVK-ZnO/GCE, (b) proportionality between μA and $t^{-1/2}$, (c) linear relationship of the conforming slopes v/s concentration (d) Tendency of Ic/I_L v/s $t^{1/2}$ for 6-TG for 0.1 – 0.5 μM/L

$$\frac{I_c}{I_L} = y^{\frac{1}{2}}\pi^{\frac{1}{2}} = \pi^{\frac{1}{2}}(k_h C_b t)^2 \quad \ldots (3)$$

Here, I_c is the oxidative current for 6-TG and I_L corresponding control run under the same set of conditions. k_h, denotes the heterogeneous rate constant, C_b is 6-TG concentration in bulk of the solution and 't' denotes run time. The linear progression of I_C/I_L *versus* $t^{1/2}$ against the 6-TG concentration furnishes K_h value of 1.058×10^5 mol^{-1} L s^{-1} as shown in Fig. 6d.

Conclusion

In this study, a new sensor comprising of ZnO Nanocomposite (Py-NVK_ZnO) has been fabricated and employed for cyclic voltammetry (CV). Impact of operative functionality on the indicators experimental for electrodic oxidation of 6-TG over Py-NVK_ZnO in comparison to neat Py-NVK coated GCE and bare GCE have been reported.

Cyclic voltammetry of electroactive species 6-TG demonstrates irreversible, diffusion-controlled mass transfer. Experiments demonstrated that Py-NVK_ZnO offers lesser resistance to charge transfer leading to higher electrocatalytic activity. Modified electrode as reported, successfully detected 6-TG in commercially available 6-TG powder in phosphate buffer of *p*H 8.2. Advantageous modifications to enhance signal efficacy for the electrocatalysis of 6-TG has been achieved and validated. Active functional moieties of Py-NVK_ZnO and 6-TG with support of large surface area of ZnO NPs furnish steady electro oxidation peak for 0.01 to 0.30 μM/L analyte strength. Sensitivity limit extends up to 0.002 μM/L further signified the efficacy and competence of the modified electrode.

Acknowledgements

The authors are thankful to Material Synthesis and Sensor Design Laboratory at Atal Bihari Vajpayee Indian Institute of Information Technology and Management, Gwalior for providing the Lab facility for the present piece of research work.

Competing Interests

The authors declare that they have no known competing financial interests or personal relationships

that could have appeared to influence the work reported in this paper.

References

1 Ibrahim MS, *Anal Chim Acta*, 443 (2001) 63.
2 Kilmartin P A, Zou H & Waterhouse A L, *J Agric Food Chem*, *49* (2001) 1957.
3 Jain R & Sharma R, *J Pharm Anal*, 2 (2012) 98.
4 Jiang D, Xiang G, Liu C, Yu J, Liu L & Pu X, *Int J Electrochem Sci*, 7 (2012) 10607.
5 Aydemir N, McArdle H, Patel S, Whitney W, Evans C W, Travas-Sejdic J & Williams D E, *Anal Chem,* 87 (2015) 5189.
6 Jain R, Tiwari D C & Shrivastava S, *Mater Sci Eng B*, 185 (2014) 53.
7 Shrivastava S, Jadon N & Jain R, *TrAC Trends Anal Chem*, 82 (2016) 55.
8 Kushwaha C S, Singh P, Shukla S K & Chehimi M M, *Mater Sci Eng B*, 284 (2022) 115856.
9 Zuman P, *FABAD J Pharm Sci*, 31 (2006) 97
10 Fedurco M, *Coord Chem Rev*, 209 (2000) 263.
11 Heinze J, *Angew Chemie Int Ed English*, 23 (1984) 831.
12 More V S, Lokhande R S, Janwadkar S P, Pitale S, Navarkar P S, Rana P & Yadav D, *INROADS- Int J Jaipur Nat Univ,* 4 (2015) 9.
13 González-Meza O A, Larios-Durán E R, Gutiérrez-Becerra A, Casillas N, Escalante J I & Bárcena-Soto M, *J Solid State Electrochem,* 23 (2019) 3123.
14 Parker V D, *Comprehensive Chemical Kinetics,* (Elsevier B.V) 1986, p. 145.
15 Amir M, Tunesi M M, Soomro R A, Baykal A & Kalwar N H, *J Electron Mater,* 47 (2018) 2198
16 Gomaa E A, Negm A & Abu-Qarn R M, *Measurment,* 125 (2018) 645.